

Wenfang Zhang · P. Schmidt-Zhang · G. Kossmehl  
W. Plieth

## Photocurrent and differential capacity measurements at polybithienyl and poly(3-butylthiophene) films

Received: 9 June 1998 / Accepted: 22 August 1998

**Abstract** Photocurrent and differential capacity measurements have been carried out at polybithienyl (PBT) and poly(3-butylthiophene) (PbUT) films on platinum. The photocurrents are cathodic, similar to inorganic p-type semiconductors. The band gap energy was determined from the photocurrent spectra ( $E_g = 1.7$  eV for PBT and  $E_g = 1.9$  eV for PbUT). The dependence of the differential capacity on the potential could be presented as Mott-Schottky plot, at least in a limited potential region. The flatband potential was determined ( $E_{fb} = 0.67$  V for PBT and  $E_{fb} = 0.58$  V for PbUT).

**Key words** Conducting polymers · Polybithienyl · Poly(3-butylthiophene) · Organic semiconductor · Differential capacity

### Introduction

The electrochemical properties, electrical conductivity and spectroscopic properties of polybithienyl films (PBT) and poly(3-butylthiophene) films (PbUT) have been extensively investigated [1–4]. In some papers, photoelectrochemical properties are mentioned [5–8]. An intensive investigation of photoelectrochemical properties was published for poly(3-methylthiophene) [9]. In the present article, investigations are presented of combined differential capacity and photocurrent mea-

surements of PBT films and PbUT films connected with tests of the stability and the electrical conductivity of these films. The paper is based on part of the results of the thesis of one of the authors [10].

### Theoretical background

The PBT and PbUT films were treated on the basis of a quasi-semiconductor model in accordance with the model of a semiconductor/electrolyte interface as suggested in the literature [11]. The potential drop  $\Delta\phi$  at the interface consists of contributions from the space charge layer  $\Delta\phi_{sc}$ , Helmholtz double layer  $\Delta\phi_H$ , and the diffuse Gouy-Chapman layer  $\Delta\phi_G$ .

$$\Delta\phi = \Delta\phi_{sc} + \Delta\phi_H + \Delta\phi_G \quad (1)$$

The corresponding differential capacity  $C_d$  at the interface between semiconductor and electrolyte includes the capacity of space charge layer  $C_{sc}$ , the Helmholtz double layer  $C_H$  and the Gouy-Chapman layer  $C_G$ . In addition to these capacities, a surface state capacity  $C_{ss}$ , parallel to the capacity  $C_H$ , may occur. Then  $C_d$  is given by

$$\frac{1}{C_d} = \frac{1}{C_{sc}} + \frac{1}{C_H + C_{ss}} + \frac{1}{C_G} \quad (2)$$

If no surface states exist and if  $C_{sc} \ll C_H, C_G$ , then

$$\frac{1}{C_d} = \frac{1}{C_{sc}} \quad (3)$$

If the potential is held in the depletion region of majority carriers, the Mott-Schottky equation for p-semiconductors holds

$$\frac{1}{C_{sc}^2} = \frac{2}{\varepsilon\varepsilon_0eN_A} \left( E - E_{fb} - \frac{kT}{e} \right) \quad (4)$$

where  $e$ ,  $\varepsilon$ ,  $\varepsilon_0$ ,  $N_A$  and  $k$  are elementary charge, semiconductor dielectric constant, vacuum dielectric

W. Zhang · G. Kossmehl  
Institute for Organic Chemistry, Free University,  
Berlin, Germany P. Schmidt-Zhang

P. Schmidt-Zhang  
Forschungsinstitut sensorik Greifswald e.v.  
Brandteichstrutse 19 17489 Greifswald

W. Plieth (✉)  
Institute for Physical Chemistry and Electrochemistry,  
Dresden University of Technology,  
Mommsenstrasse 13,  
D-01062 Dresden, Germany  
e-mail: plieth@cech01.chm.tu-dresden.de

constant, doping level of the p-semiconductor with acceptor states and Boltzmann constant, respectively.  $E - E_{fb} = \Delta\phi_{sc}$  is the electrode potential relative to the flat-band potential which can be determined by the Mott-Schottky plot.

When a p-semiconductor is immersed into an electrolyte containing a redox pair, whose Fermi level is higher than the p-semiconductor Fermi level, a band bending appears at the semiconductor surface. If this surface is illuminated by light with a wavelength of  $\lambda$  and with energy  $h\nu > E_g$  (band gap energy), the photoholes move to the bulk and the photoelectrons to the surface. A reduction reaction occurs at the semiconductor surface, leading to cathodic photocurrents.

This photocurrent was described first by Gärtner [12], then by Butler [13] who simplified the expression given by Gärtner. He gave the following equation:

$$i_{ph} = e\phi_0 \left( 1 - \frac{\exp(-\alpha W_0 (E - E_{fb})^{1/2})}{1 + \alpha L_p} \right) \quad (5)$$

Here  $i_{ph}$ ,  $\alpha$ ,  $W_0$ ,  $\Phi_0$ , and  $L_p$  are photocurrent density, monochromatic absorption coefficient, thickness of the depletion layer, total photon flux and diffusion length of minority carriers, respectively. For  $L_p \ll 1$  and  $\alpha W_0 (E - E_{fb})^{1/2} \ll 1$  the following approximation is obtained:

$$i_{ph}^2 = (e\phi_0 \alpha W_0)^2 (E - E_{fb}) \quad (6)$$

whereby the  $i_{ph}^2/E$  plot is linear, and the flat-band potential can easily be determined from the intersection point with the  $E$ -axis.

## Experimental

### Equipment

The equipment used for the electrochemical measurements and synthesis of the PBT and PBUt films is described in detail in a preceding paper [14]. The working electrode (WE) was a platinum disc with an area of 0.071 cm<sup>2</sup>. A twisted platinum wire, larger in area than the WE, was used as a counter electrode (CE). The reference electrode (RE) was Ag/AgCl for organic electrolytes and a saturated calomel electrode (SCE) for aqueous electrolytes, respectively. A platinum electrode, divided into two parts, was used for the measurement of the electrical conductivity [15].

The capacity was measured by means of a two-phase lock-in amplifier (model 278 EG&G). The modulation frequencies were 20, 30, 150, 400, 900 and 1500 Hz. For photocurrent measurements a photoelectrochemical cell with a quartz window, a monochromator with wavelengths ranging from 250 nm to 1500 nm and a light chopper working at a frequency of 0.1 Hz were used. An argon plasma lamp served as the light source with a nearly constant intensity in the experimental spectral region. The photocurrent was amplified by the lock-in amplifier and recorded by a  $x$ - $y$  recorder (Linseis).

### Chemicals

Commercially obtained bithienyl and butylthiophene were purified by chromatography. Propylene carbonate of spectrophoto-

metric grade, acetonitrile (p.a.) and tridistilled water were used as solvents; LiClO<sub>4</sub> (p.a.), KCl (p.a.), HCl (p.a.) and NaOH (p.a.) were used as supporting electrolytes.

## Results and discussion

### Stability and electrical conductivity of PBT and PBUt films

PBT films were prepared by cyclic voltammetry (CV) in propylene carbonate/0.1 M LiClO<sub>4</sub> (Fig. 1), PBUt films by CV in acetonitrile/0.1 M LiClO<sub>4</sub>. The concentration of bithienyl and butylthiophene was 0.01 M. The stability of the PBT and PBUt films in aqueous electrolytes with different pH values was tested by CV. During cycling of the potential the PBT film remained stable. The PBUt film was stable only in neutral and alkaline electrolytes. In an acidic electrolyte, higher cathodic currents, caused by the evolution of hydrogen at the surface of the platinum electrode, were observed. The film was unstable under these conditions.

The electrical conductivity of PBT and PBUt films was determined in situ by means of a platinum electrode divided into two parts [15]. A dry oxidized PBT film and a dry oxidized PBUt film have an electrical conductivity of 0.2 S/cm and 7 S/cm, respectively, similar to the results in the literature [16, 17]. The measurements were repeated over a period of 6 days, giving constant results. When the PBT and PBUt films were wet, their electrical conductivities were higher than in the dry state.

The electrical conductivity of the PBUt film was higher than that of the PBT film, but the PBUt film had a lower degree of oxidation than the PBT film. The explanation is given by the butyl substituent in the 3-position of the thiophene molecule. This substituent affects the space structure of the polymer film, decreasing the doping level and increasing the mobility of the electrons in the PBUt film [18, 19].

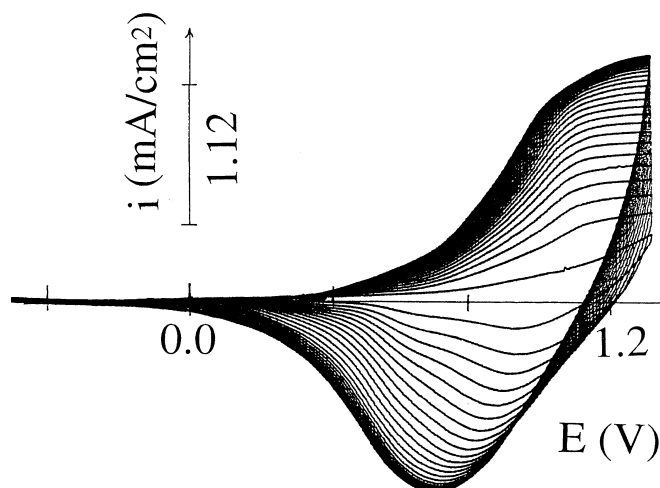


**Fig. 1** Growths of a PBT film by cyclic voltammetry in propylene carbonate/0.1 M LiClO<sub>4</sub>/0.01 M BT ( $E$  vs. Ag/AgCl)

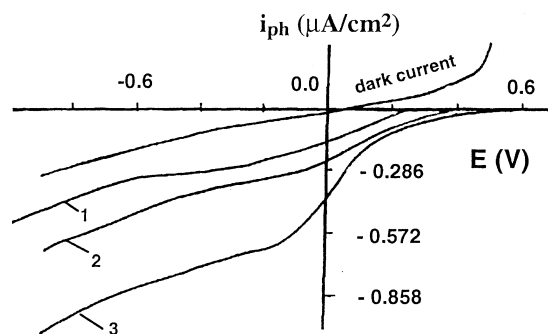


**Fig. 2**  $i_{ph}/E$  curves of a PBT film in  $H_2O/0.2$  M  $LiClO_4$  electrolyte at different pH values: 1, 7.04; 2, 4.16; 3, 2.58;  $\lambda = 460$  nm

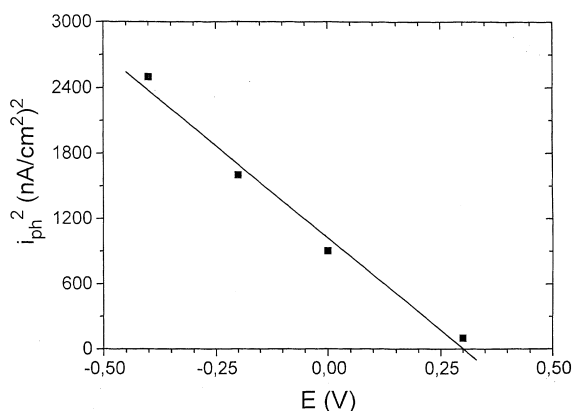


**Fig. 3**  $i_{ph}^2/E$  plot of a PBT film in  $H_2O/0.2$  M  $LiClO_4$  electrolyte at pH 7.04;  $\lambda = 460$  nm, corresponding to Fig. 2

#### Photocurrent-potential ( $i_{ph}/E$ ) measurements at the PBT film

The  $i_{ph}/E$  curves of a PBT film ( $\lambda = 460$  nm) are shown in Fig. 2. A cathodic photocurrent with a limiting current in the potential range from 0.2 V to  $-0.4$  V is observed. The potential range corresponds to the reduced form of the polymer. The cathodic current is typical for a p-semiconductor. The photocurrent limit does not remain constant and rises during progression of the cathodic potential sweep. At constant potential the cathodic photocurrent increases with a decreasing pH value. This behaviour corresponds with the dependence of the flat-band potential on the pH as described below.

For the PBT film and in a small potential range ( $E_{fb} - E = 0.5$  V) the square of the photocurrent,  $i_{ph}^2$ , is directly proportional to the electrode potential  $E$  (Fig. 3). From the slope of the  $i_{ph}^2/E$  line the optical flat-band potential  $E_{fb}$  can be evaluated according to Eq. 6 [9]. The flat-band potential of the PBT film depends linearly on the pH value (30 mV/pH) (Fig. 4).

#### Photocurrent spectra at the PBT and PBuT films

The photocurrent spectra of a PBT and a PBuT film measured at different potentials are shown in Figs. 5 and 6.

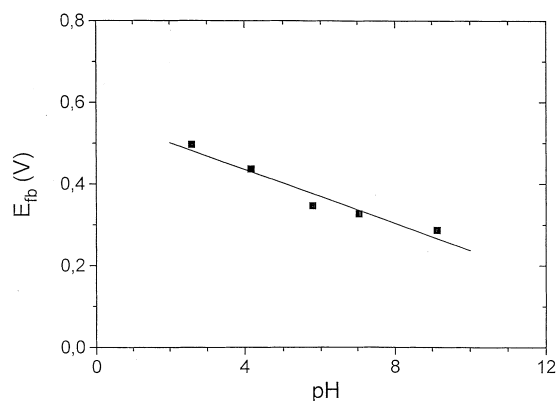


**Fig. 4** Dependence on the pH value of the optical flat-band potential of a PBT film in  $H_2O/0.2$  M  $LiClO_4$

The photocurrent spectra show a current maximum at a wavelength of 460 nm ( $h\nu = 2.70$  eV) for the PBT-film and of 450 nm ( $h\nu = 2.76$  eV) for the PBuT film. These photocurrent maxima are similar to those of UV/VIS absorption spectra for corresponding films [20]. The photocurrent maxima correspond with the  $\pi-\pi^*$  transition from the LUMO to the HOMO of the polymer chains [21, 22]. In the semiconductor approximation this can be described as a transition from the valence band to the conduction band. The feature of the photocurrent is an image of the distribution of electronic energy levels in

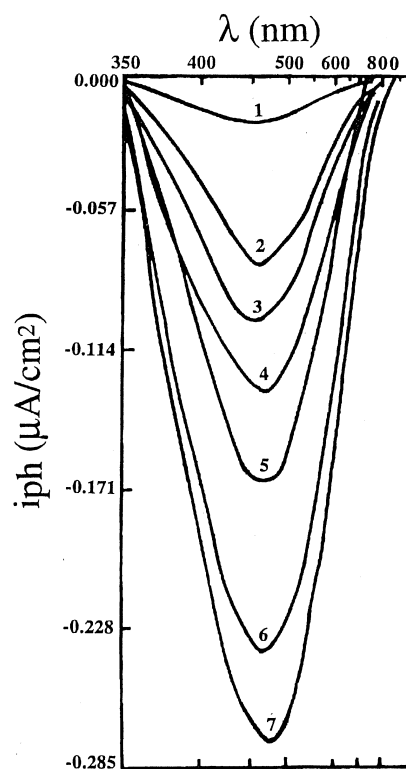


**Fig. 5** Photocurrent spectra of a PBT film at different potentials in  $H_2O/0.2$  M  $LiClO_4$ , pH = 7.0;  $E = +0.3$  V (1), 0.0 V (2),  $-0.2$  V (3),  $-0.4$  V (4),  $-0.6$  V (5),  $-0.8$  V (6),  $-1.0$  V (7)

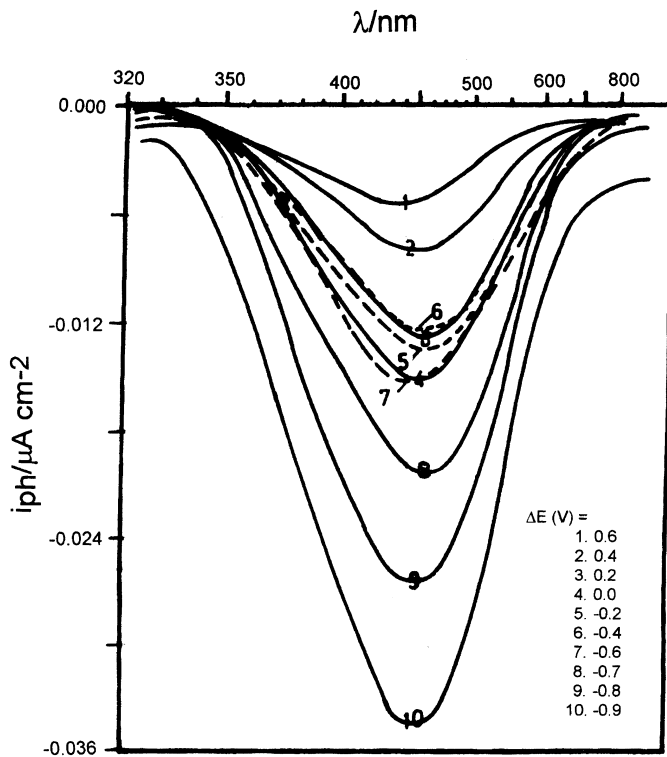


Fig. 6 Photocurrent spectra of a PBT film at different potentials in  $\text{H}_2\text{O}/0.2 \text{ M LiClO}_4$ ; pH = 7.0:  $E = +0.6 \text{ V}$  (1),  $+0.4 \text{ V}$  (2),  $+0.2 \text{ V}$  (3),  $0.0 \text{ V}$  (4),  $-0.2 \text{ V}$  (5),  $-0.4 \text{ V}$  (6),  $-0.6 \text{ V}$  (7),  $-0.7 \text{ V}$  (8),  $-0.8 \text{ V}$  (9),  $-0.9 \text{ V}$  (10)

the polymer. Figures 5 and 6 could be explained by an approximately Gaussian distribution. The band gap of the polymer film ( $E_g$ , approximately the long wavelength limit of the  $i_{ph}$  spectrum) can be estimated from Figs. 5 and 6. One obtains:

$$E_g = 1.7 \text{ eV } (\lambda = 778 \text{ nm}) \text{ for the PBT film}$$

$$E_g = 1.9 \text{ eV } (\lambda = 651 \text{ nm}) \text{ for the PBT film}$$

The values are smaller than those reported for polythiophene and polymethylthiophene [20].

### Differential capacity $C_d$

#### Differential capacity of the PBT films

The dependence of the differential capacity on the potential ( $C_d/E$  curve) and the  $C_d^{-2}/E$  curve for a PBT film (thickness  $d = 1.3 \mu\text{m}$ ) are shown in Figs. 7 and 8. An ideal linear behaviour in the Mott-Schottky plot cannot be observed. In a rough approximation, an almost linear potential region between  $0.4 \text{ V}$  and  $0.6 \text{ V}$  was identified. The line is comparable to the other observations made and is therefore interpreted as the Mott-Schottky line.

The negative sign of the line means that the PBT film can be treated as a p-semiconductor and the theory for inorganic semiconductor/electrolyte interfaces can be tentatively applied to the polymer film/electrolyte inter-

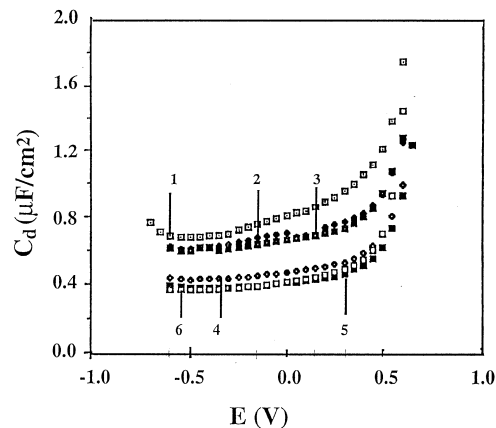


Fig. 7  $C_d/E$  curves at different frequencies of a PBT film in  $\text{H}_2\text{O}/0.2 \text{ M LiClO}_4$ , pH = 7.0;  $f = 20 \text{ Hz}$  (1),  $80 \text{ Hz}$  (2),  $150 \text{ Hz}$  (3),  $450 \text{ Hz}$  (4),  $900 \text{ Hz}$  (5),  $1500 \text{ Hz}$  (6)

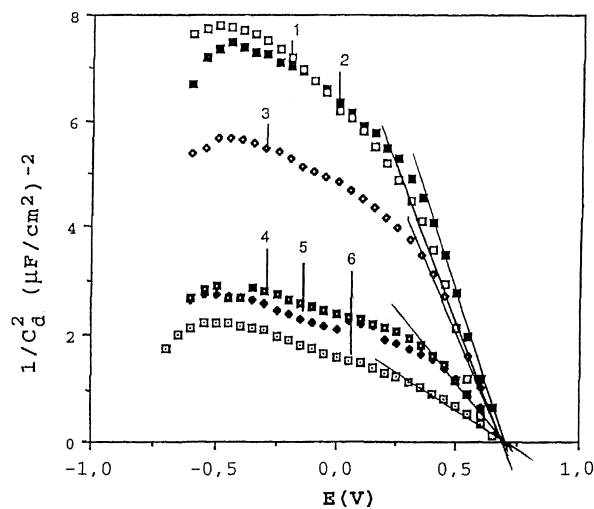


Fig. 8  $C_d^{-2}/E$  curves (Mott-Schottky plots) corresponding to Fig. 7;  $f = 1500 \text{ Hz}$  (1),  $900 \text{ Hz}$  (2),  $450 \text{ Hz}$  (3),  $150 \text{ Hz}$  (4),  $80 \text{ Hz}$  (5),  $20 \text{ Hz}$  (6)

face. The flat-band potential for the PBT film can be determined by the intersection point of the Mott-Schottky line with the  $x$ -axis. A value  $0.67 \text{ V}$  is obtained, more positive than the optical flat-band potential (see above). Such a difference is also found for inorganic semiconductors and is explained by quenching of the photoelectrochemical excitation at surface states.

The differential capacity  $C_d$  decreases with increasing modulation frequency  $f$ . This dependence follows the equation

$$C_d^{-1} = \kappa(E) \log f + A \quad (7)$$

where  $A$  is a constant. The  $C_d^{-1}/\log f$  plot is linear in the frequency range from  $100 \text{ Hz}$  to  $3 \text{ kHz}$  (Fig. 9) and its slope depends on the electrode potential. Equation 7 is similar to the equation given by Dutoit et al. [23], which describes a frequency dependence of the capacity at CdSe, CdS and  $\text{TiO}_2$  semiconductors, respectively. The

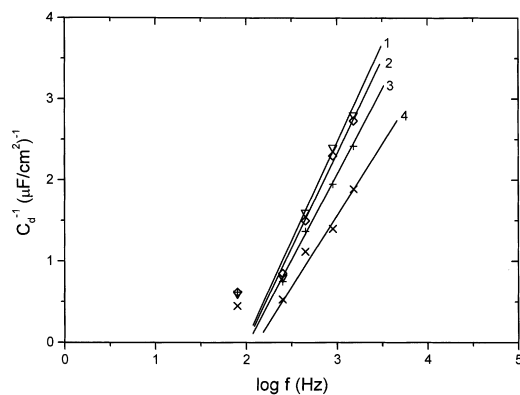


**Fig. 9** Frequency dependence of the capacity for the PBT film in Fig. 8; potential  $E = -0.6$  V (1),  $-0.35$  V (2),  $0.15$  V (3),  $0.3$  V (4)

frequency dependence has been interpreted as a consequence of the structure defects on the surface region of the electrode. This can be described by a surface state capacity  $C_{ss}$  parallel to the capacity of the space charge layer  $C_{sc}$  [11, 23, 24]. The frequency dependence of  $C_d$  has the consequence that the slope of the Mott-Schottky plots varies with the modulation frequency, similar to typical inorganic semiconductors like Si, GaAs, GaP and  $\text{TiO}_2$  [25, 26].

The  $C/E$  curves in Fig. 8 show a plateau in a wide potential range instead of a single minimum of the capacity. This can be explained by the fact that the density of doping (remaining  $\text{ClO}_4^-$  anions in the film) is extremely high (of the order of  $10^{20}$ – $10^{21}$   $\text{cm}^{-3}$ , obtained from the slope of the Mott-Schottky line). As in the case of inorganic semiconductors, the plateau of the capacity is explained by very high doping densities because the equilibrium of the minority carriers cannot be established [11, 24].

#### Differential capacity measurements at PBUt films

A similar behaviour was observed for PBUt. At frequencies above 1 kHz the decay of the  $C_d^{-2}/E$  plots at more positive potentials can be interpreted approximately as being a type of Mott-Schottky line. The negative slope of this line again indicates the behaviour of a p-semiconductor. The flat-band potential for the PBUt film is 0.58 V. The slopes of the Mott-Schottky plots depend on the frequency, similar to that of the PBT film.

#### Discussion

The application of concepts of semiconductor electrochemistry to the PBT and PBUt films showed a remarkable correspondence quite unexpectedly if one regards the critical comments in the literature on highly disordered systems (e.g. [27]). The following points confirm this interpretation:

1. A cathodic photocurrent was observed for PBT and PBUt.
2. Linear  $i_{ph}2/E$  regions at the PBT films gave the optical flat-band potential, 0.3 V at  $\text{pH} = 7$ , depending on the pH.
3. The majority of  $C/E$  measurements at PBT and PBUt films were similar to those measured at p-type semiconductors; at least in a limited potential region, the presentation of the data as Mott-Schottky plots was possible.
4. The sign of the slopes of the Mott-Schottky plots was equal to that of p-type semiconductors.
5. Mott-Schottky plots gave flat-band potentials of 0.67 V (PBT) and 0.58 V (PBUt).

If one is using as a rough estimate a value of the dielectric constant of the polymers of  $\epsilon = 10$  [29], a doping density can be calculated from the Mott-Schottky plots, giving the order of magnitude of  $10^{20}$ – $10^{21}$  (1 kHz).

The limited linear region of the Mott-Schottky plots and the high doping density show that the investigated polymers are highly disordered materials. Suggestions were made for a different treatment of such materials [27]. Derivations for highly doped materials may also be the effect of increasing degeneracy of the energy levels of the charge carriers [30]. In the meantime, films with more regular structure could be prepared [28] which confirm the treatment of the reduced state of these polymers by the simple semiconductor model.

#### References

1. Chung T-C, Kaufmann JH, Heeger AJ, Wudl F (1984) *Phys Rev B* 30: 702
2. Roncali J, Garnier F, Lemaire M, Garreau R (1986) *Synth Met* 15: 323
3. Lapkowski M, Zagorska M, Kulszewicz Bajera I, Koziel K, Pron A (1991) *J Electroanal Chem* 310: 57
4. Kaeriyama K, Sato M, Tanaka S (1987) *Synth Met* 18:233
5. Stöckert D, Kessel R, Schultze WJ (1991) *Synth Met* 41–42: 1295
6. Fang Y, Chen LA, Chu LM (1991) *Synth Met* 52: 261
7. Morgenstern T, König U (1994) *Synth Met* 67: 263
8. Greenwald Y, Cohen G, Poplawski J, Ehrenfreund E, Speiser S, Davidov D (1995) *Synth Met* 69: 365
9. Paramunge D, Tomkiewicz M, Ginley D (1990) *J Electrochem Soc* 134: 1384
10. Zhang W (1994) Thesis, Free University, Berlin
11. Gerischer H (1970) In: Eyring H, Henderson D, Jost W (eds) *Physical chemistry, an advanced treatise*, vol IXA. Academic Press, New York, p 463
12. Gärtner W (1959) *Phys Rev* 116: 84
13. Butler MA (1977) *J Appl Phys* 48: 1914
14. Zhang W, Plieth W, Kossmehl G (1997) *Electrochim Acta* 42: 1653
15. Kossmehl G, Fechner D, Plieth W, Zhang W, Zerbino I (1990) In: von Sturm F (ed) *Werkstoffe in der Elektrochemie* (Dechema monograph, vol 121) VCH, Weinheim, p 279
16. Drury MA, Seymour RJ, Tripathy SK (1994) In: Davidson T (ed) *Polymers in Electronics*. (ACS Symposium Series No 242) American Chemical Society, Washington, p 473

17. Kulszewicz-Bajer I, Pawlicka A, Plenkiewicz J, Pron A (1989) *Synth Met* 30: 355
18. Waltman RJ, Gargon J, Diaz AF (1983) *J Phys Chem* 87: 1459
19. Butler MA, Ginney DS (1977) In: Heller A (ed) *Semiconductor-liquid junction solar cells. Proceedings – Conference Airlie Va*, Electrochemical Society, Princeton NY, p 290
20. Druy MA, Seymour RJ (1983) *Org Coat Appl Polymer Sci Proc* 48: 561
21. Izdinov SO (1968) *Soviet Electrochem* 4: 927
22. Tourillon G (1986) In: T. A. Skotheim (ed) *Handbook of conducting polymers*, vol 1. Marcel Dekker, New York, Basel p. 293
23. Dutoit EC, Van Meirhaeghe RL, Cardon F, Gomes WP (1975) *Ber Bunsenges Phys Chem* 79: 1206
24. Westfahl J, Landsberg R, Janiez P (1977) *Elektrokhimiya* 13: 640
25. Haag T (1984) Thesis, Free University, Berlin, p 56
26. Byker HJ, Wood VE, Austin AE (1982) *J Electrochem Soc* 129: 1982
27. Gerischer H (1990) *Electrochim Acta* 35: 1677
28. Fikus A, Rammelt U, Plieth W (1998) *Electrochim Acta* 44: (in press)
29. Scherbel J, Nguyen PH, Paasch G, Brüttling W, Schwoerer M (1998) *J Appl Phys* 83: 5045
30. Paasch G, Nguyen PH, Fisher A (1998) *Chem Phys* 227: 219